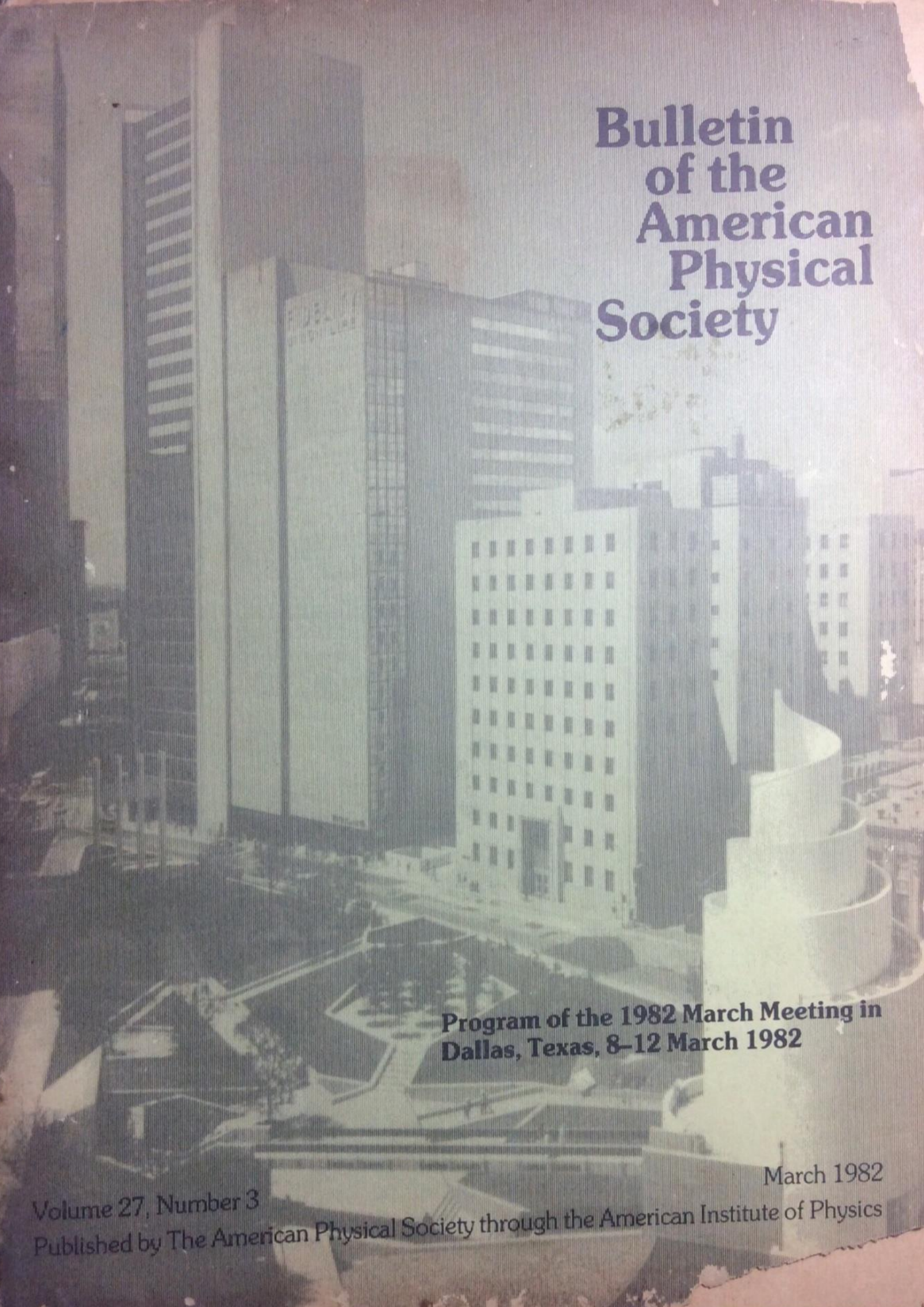

Bulletin of the American Physical Society

Program of the 1982 March Meeting in Dallas, Texas, 8–12 March 1982

March 1982

Volume 27, Number 3

Published by The American Physical Society through the American Institute of Physics

SESSION GY: POSTER SESSION
Wednesday morning, 10 March 1982
Royal Room, Fairmont Hotel at 10:30 A.M.

GY 1 A New Transient Phenomenon Associated with Photostimulated Exoelectron Emission.* H. SHIGEKAWA and S. HYODO, Univ. Tokyo. -- When photoillumination is interrupted, the exoelectron emission from scratched metal samples decay quickly; when the illumination is resumed, however, the recovered exoelectron emission shoots up to a value significantly higher than before and then decreases gradually. -- a fact overlooked by previous authors[1]. This transient phenomenon has been studied in some detail as a function of the interval of the interruption and photon energy. To explain our data we propose a model that there are two excitation process competing during PSEE; one is the photoexcitation of the electrons at defects-related energy levels above the Fermi level and the other is the thermal exciatation of the lower lying electrons to the empty defect-related levels. The rate equations based on this model explain our observations to a satisfactory extent.

*Submitted by T. SAKURAI.

1.D.R. Arnott and J.A. Ramsay, Surface Science 28, 1 (1971).

GY 2 Model Calculations of the Effective EXAFS and EAPFS Phase Factors for Br_2, Al_2O_3, and SiO_2. G.E. LARAMORE*, Dept. Radiation Oncology, University of Washington--Model calculations are made for the effective EXAFS phase factor for excitation of the 1s level in Br_2. A comparison is made between nonselfconsistent potentials constructed from atomic Br and ionic Br^{1+} (1s hole) charge densities and for fully selfconsistent potentials determined using the SCF-Xα-SW method. The effect of screening charge transfer is described. Calculations are also presented for the lowest-lying $\sigma \rightarrow \sigma^*$ and $\pi \rightarrow \pi^*$ excited states in Br_2^{1+} (1s hole). The effective phase factor is calculated as a function of momentum over the range $0.5\text{Å}^{-1} \leq k \leq 16.2\text{Å}^{-1}$ corresponding to energies to ∿1000eV above the absorption edge. All of the calculated curves have similar slopes for $k \geq 6\text{Å}^{-1}$ but their behavior differs significantly for lower momentum values. Nonselfconsistent calculations are presented for the effective EXAFS and EAPFS phase factors for excitation of the O 1s level in clusters corresponging to bulk Al_2O_3 and SiO_2. Again is noted a breakover between a low-momentum and a high-momentum behavior but this time the changeover occurs between $3\text{-}4\text{Å}^{-1}$. The implications of this for surface EXAFS measurements are discussed.
*Supported in part by ONR Contract N00014-79-C-0371

GY 3 The Solvent Effect in Enzyme-Substrate Interactions: Models of Carboxypeptidase. C.A. Venanzi, H. Weinstein, Mt. Sinai Medical School, CUNY, G. Corongiu, and E Clementi, IBM Poughkeepsie--The structure of water in the active site of carboxypeptidase A is studied with ab initio quantum mechanical calculations and the Monte Carlo statistical method. The zinc-containing portion of the active site was modelled by $[Zn(NH_3)_2(OH)]^+$ in a geometry taken from the crystal structure of the enzyme. The potential energy surface was probed by calculating the interaction energy of the model with a water molecule situated at 211 representative positions. Energy points were fit to an analytical expression which was used to determine cross-sectional contour maps of one water molecule moving on the fitted potential energy surface. Expansion of the model to include other catalytically important functional groups showed the specific contribution of each to the interaction potential. This work is a pilot study for a Monte Carlo simulation of the solvent structure in the 50-amino acid active site of carboxypeptidase A[1] under the conditions: (1) native enzyme and (2) enzyme bound to the substrate glycyltyrosine.
Supported by grants from the National Institute on Drug Abuse: #5-132-DA-07135 (CAV) and DA-00060 (HW).
[1]Crystal structure by W.N. Lipscomb, et al., Brookhaven Symposium 21, 24 (1968).

GY 4 Protein Conformation From Electron Spin-Lattice Relaxation Data.* J. P. Allen, J. T. Colvin, and H. J. Stapleton, University of Illinois at Urbana-Champaign. Electron spin relaxation data from five low spin ferric proteins are presented as evidence that the fractal model of Stapleton et. al. (1) accurately describes the temperature dependence observed in these biopolymers. This model relates protein structure, as characterized by a fractal dimension d (2), and the density of vibrational states $\rho(\omega)$, which varies as $\omega^{**}(d-1)$, to the temperature dependence of the Raman relaxation rate, which then varies as $T^{**}(3+2d)$. X-ray data from several proteins indicate they are characterized by non-integer values of d which range from about 1.32 to 1.86, thus bracketing the 1.67 value associated with a self-avoiding random walk in three dimensional space. Relaxation data from ferricytochrome c and ferredoxin yield d values of 1.67(3) and 1.34(6), respectively, in agreement with x-ray data from which d values of 1.66(5) and 1.34(5) can be computed. Although d is but a single structural parameter, it is nevertheless a useful indicator of protein conformation.
* Supported by the USPHS under NIH Grant 24488.
(1) H. J. Stapleton et. al. Phys. Rev. Let. 45, 1456 (80)
(2) B. B. Mandelbrot, "Fractals" (Freeman, 1977).

GY 5 Resonance Raman Detection of Structural Dynamics at the Active Site In Hemoglobin. D. L. ROUSSEAU, M. R. ONDRIAS, Bell Laboratories, and S. R. SIMON, SUNY, Stony Brook - The low frequency (100-500 cm^{-1}) resonance Raman spectra of various hemoglobins, isolated α and β subunits, and model 2-methylimidazole heme complexes have been obtained at 77K. All hemoglobin species have nearly equivalent spectra under these conditions suggesting that quaternary structure dependent differences are not maintained at low temperature. The temperature dependence of the deoxyhemoglobin spectrum was examined over the range of 10-300K. Of particular interest is the behavior of the band assigned as the iron-histidine stretching mode. It displays a large change in frequency and width upon lowering the temperature from 300 to 10K. The temperature dependence of the data indicates the presence of dynamic processes. The dynamics of this mode in frozen hemoglobins can be qualitatively and quantitatively described as vibrational dephasing via anharmonic coupling to other vibrations of the heme-imidazole system.

GY 6 Rotational Motion of the NH_4^+-Tetrahedron in NH_4Cl. R. W. GERLING*+, U. of Georgia and A. HÜLLER, U. of Erlangen-Nürnberg, W. Germany - We have treated the rotational motion of the NH_4^+-group in the framework of the Langevin-equation. Hüller and Kane calculated the rotational potential from an electrostatic point charge model.[1] There is excellent agreement between their theoretical and experimental results for the librational frequencies. Nevertheless their predictions disagree with the results from neutron scattering experiments.[2] By mapping the rotational motion of the tetrahedron on the motion of a point on the 4-dimensional unit sphere we have derived a Langevin-equation. Detailed information about the jump dynamics can be extracted from the numerical solution of this Langevin-equation. We found that multiple jumps play an important role. Using multiple jumps as well as single jumps we can explain the neutron scattering experiments without using adjustable parameters.

*On leave from U. of Erlangen-Nürnberg, W. Germany.
+Supported in part by a Fulbright Travel Grant.
[1]A. Hüller, J. W. Kane, J. Chem. Phys. 61, 3594 (1974).
[2]J. M. Töpler et al., J. Chem. Phys. 69, 3170 (1978).

GY 15 Moire Topography for the Measurement of Angle of Spinal Curvature in Three Dimensions. S. A. KAMAL, Indiana U., Bloomington—Cobb's angle can be measured from two dimensional roentgenograms. It gives information about scoliosis. If there is kyphosis or lordosis in addition to scoliosis, it is necessary to define three dimensional angle. In this paper three dimensional angle is defined in terms of direction cosines of the spine. A relation is derived connecting three dimensional angle to Cobb's angle. The spinal deformity may be partially or completely corrected by asking the patient to hang freely. After passive correction angle can be measured from posterio-anterior and lateral X-rays. The angle between the old and new spinal position can therefore be calculated. The degree of deformity is defined in terms of this angle. Cobb's angle can also be measured from moire topographs[1,2]. This paper gives a method to measure three dimensional angle by moire topographs.

[1] S. A. Kamal, Measurement of the Angle of Spinal Curvature by Moire Topographs, JIMA(Florida), to be published.

[2] M. M. El-Sayyad and S. A. Kamal, Cobb's Angle Measurement by Moire Topographs, 34th Annual Conference on Engineering in Med. & Biol., 1981, Houston, Texas.

GY 16 A New Process for Patient Alignment. S. A. KAMAL, Indiana U., Bloomington—Proper patient alignment is necessary for moire topography. To align the patient a 10 x 10 cm mirror is fixed to two plastic strips. The strips are provided with a belt so that they can be attached to patient's sides. We take z-axis perpendicular to floor, y-axis passing through the midpoint of the mirror (attached to the patient) and perpendicular to it. A 10 x 10 cm wooden plate is held fixed in the xz-plane and the mirror is 20 cm away from this plate. The mirror should also be in xz-plane. x-axis is perpendicular to z-axis and passes through the plate. Lamp L1 is on (-z)-axis and tilted upwards. Lamp L2 is on (x)-axis and tilted to the left. The lights from both the lamps fall on the mirror and reflected back on the scale. When light from L1 falls on (z)-axis and from L2 falls on (-x)-axis, the patient is ready for moire topography. For the photograph of the back, the equipment is fixed on chest/stomach and sides and vice versa. The process presented here is simple, easy to perform and cheap.

GY 17 [illegible] SPACE A DIRECT DEDUCTION [illegible] — S.M. Ayub, A-2, Bliss Apartments, 4/1 Nc Neil Road, Karachi/Pakistan—In conventional concepts 'S' has three dimensions; this is established for Reimannian 'S' in General Relativity with the furthered concept of equivalence of $S \equiv T$ at the fringe of the universe, and the reversibility of the Reimannian and Energy Tensors in A. Einstein's Equation. Applying this, the Tensor Equation becomes $3R_{\mu\nu} = g_{\mu\nu}$. In terms of comparative equality, G functions therefore in a minimum Reimannian 'S' of three dimensions. The above is established consequently for 'T', if ≥ 0 or 1. For dimensions, these could be n for 'S' if $n > 3$, theoretically. This inherent conclusion would appear to be interesting, as it has been reached without any pre-knowledge of 3 dimensionality in the continuum.

GY 18 [illegible] IN [illegible] — S.M. Ayub, A-2, Bliss Apartments, 4/1 Nc Neil Road, Karachi / Pakistan—Laws of symmetry demand that if 'C' could decrease, it could also increase under specified conditions. This was arrived at by visualising two spaces, one with 'C' and the other with $\sqrt{-1}$ 'C' where velocities $>>$ c. 'C' assumed very high values in high fields. This was proven by Relativistic Energy Equation and alternately by Maxwellian Equations of the second order where $\sqrt{-1}$ C functioned in the second space. The estimated field was 10^{18} - 10^{17} eV, nearabout P binding energy. Present accelerations do not go beyond nearly 10^{12} eV, and the requisite field exists naturally in space. This is also supported by the velocity of matter/energy reaching [illegible] even now at the fringe of the Universe after 'Big Bang'. This is also supported by the newly developed concept of fusion of Space/Time at the Universe fringe, and the reversibility of Reimannian/Energy Tensors in the Relativity Equation, which theoretically yields the value of 'C' between 0 and ∞. The concept has applications in Power Reactors with proper artifices.

*A.P.S. Bulletin, April, 1981, A7-15

GY 19 'C' a [illegible] IS PRESENT — S.M. Ayub, A-2, Bliss Apartments, 4/1, Nc Neil Road, Karachi/Pakistan— with the decelerating Universe fringe, although an average is taken for its expansion, the complete fusion and identity of Space/Time, and the reversibility of Reimannian/Energy Tensors, A. Einstein's Equation $R_{\mu\nu} - \frac{1}{2} g_{\mu\nu} = \frac{8\pi G}{c^4} T_{\mu\nu}$ (Standard notations) yields $\frac{1}{2} g_{\mu\nu} = k_{\mu\nu} \times$ Constant or ε is expressible as $\frac{1}{2} R_{\mu\nu}$ dimensionally. As $T_{\mu\nu}$ involves 'C', G is non-existent if 'C' is zero. But the conclusion that G is generated by Reimannian 'S' structural pattern (R being there), as envisaged by A. Einstein is established by the present concept of equivalence of Space/Time in normal conditions, for definite.

GY 20 'C' [illegible] IN NUCLEAR FIELDS BY DIRECT [illegible] — S.M. Ayub, A-2, Bliss Apartments, 4/1 Nc Neil Road, Karachi/Pakistan— Various methods proved that the value of 'C' lowers down to 10^{8} cms./sec. to $10^{7.5}$ cms./sec. in nuclear fields. In a paper drawn up in 1957, published in January 1958, the method used was the exchange of K_o alternately with mesons (and the rotation of the Nuclear Molecule to reduce α, the coupling constant) between nucleons. The Uncertainty Principle was used, and second method was to use Hermitian Operators, taking 'Y' to be the Isospin Invariant of 'e'. Similar conclusions were drawn by electrodynamical propagation of [illegible] waves and by General Relativity derivations. It was mentioned that the verification could be made by Linear accelerators and also in Synchrocyclotrons in which more matter will result from the measured quanta of Energy in high fields. The concept could have practical applications in Power Reactors.

* Fundamental Particles, Pak. Jour. Sci. Jan. 1958, S.M. Ayub.

** New Concepts of Time and Breakdown of the Law of Conservation of Mass/Energy in Nuclear Fields.. Journ. of Nat. Sci. and Maths., Vol. XII, No. 1, April, 1972 (drawn up in 1969) and other papers.

GY 21 Extrusion Of Mountain Ridge Systems. KEITH L. MCDONALD, P. O. Box 2433, Salt Lake City, Ut.—We have found no examples in which 4 or more long running ridges intersect, while mountain peaks or knolls occur where 3 such ridges intersect. An ideal extruded ridge is defined by its running crest that is flanked on each side by a subparallel (sensibly) vertical fault. Thus if a broad ridge or mountain base has a sequence of crests separated by erosion gullies (often 100 m or more deep), the crests are not counted as ridges owing to absence of the sets of faults. Photo (Oct. 1980): viewing over Catherine Knoll, 0.37 km along ridge WNW from Sunset Peak (shadow), down Little Cottonwood Canyon; n-s oriented Albion Basin Ridge intersects at terminus of n, main ridge of Big Cotton Canyon. This n. main ridge veers [illegible] direction. Twin Peaks are 2nd, 3rd peaks [illegible] to a final W. [illegible] Pk. of canyon mouth [illegible] Squirrh, Stansbury Mts. appear.

MOIRÉ TOPOGRAPHY FOR THE MEASUREMENT OF ANGLE OF SPINAL CURVATURE IN THREE DIMENSIONS*

SYED ARIF KAMAL†

Department of Physics, Indiana University, Bloomington, Indiana 47405, U.S.A.

KEY WORDS

moiré topograph, spinal curvature, passive test, Cobb's method, scoliosis, kyphosis, Asr angle

The measurement of angle is an important step in the evaluation of spinal deformity. The spinal curve is measured either by Cobb's or Risser-Ferguson's method[1]. These methods are applicable for two dimensional roentgeneograms and give information about the curve due to scoliosis. If there is kyphosis or lordosis in addition to scoliosis, Cobb's or Risser-Fergusen's method does not give full information. It is necessary that angle of spinal curvature is defined in three dimensions. The three dimensional angle, named as 'Asr Angle'[2] is defined in terms of direction cosines of the spine.

Consider a vector $\vec{ML}$ making an angle α with the x-axis, β with the y-axis and γ with the z-axis. I have

$$\cos^2\alpha + \cos^2\beta + \cos^2\gamma = 1 \qquad (1)$$

If $\vec{ML}_0$ is another vector having direction cosines $\cos\alpha_0$, $\cos\beta_0$, $\cos\gamma_0$

*Updated version.

†Present address: Dept. of Physics & Astronomy, The Johns Hopkins Univ., Baltimore, MD 21218.

Homepage: https://www.ngds-ku.org/kamal
e-mail: profdrakamal@gmail.com

Bull. Amer. Phy. Soc. **27 (3)**, 301: abstract#GY15

and $\phi = \angle LML_0$, I have

(2) $$\cos\phi = \cos\alpha\cos\alpha_0 + \cos\beta\cos\beta_0 + \cos\gamma\cos\gamma_0$$

The projections of $\vec{ML}$ on x-, y-, z-axes and xy-, yz-, zx-planes can be written as (Fig 1)

(3a) $$ML_x = ML\cos\alpha, \quad ML_y = ML\cos\beta, \quad ML_z = ML\cos\gamma$$

(3b) $$ML_{yz} = ML\sin\alpha, \quad ML_{zx} = ML\sin\beta, \quad ML_{xy} = ML\sin\gamma$$

In the case of scoliosis, the angle of lateral deviation of spine can be measured from posterio-anterior roentgenogram. The angle of spinal curvature θ can be expressed as (Fig 2)

(4) $$\theta = \gamma_1 + \gamma_2$$

The railroad sign line in Fig 2 represents the position of spine. Further note that

(5a,b) $$\beta_1 + \gamma_1 = 90^0 = \beta_2 + \gamma_2, \qquad \alpha_1 = 90^0 = \alpha_2$$

Therefore

(6a) $$\cos^2\alpha_1 + \cos^2\beta_1 + \cos^2\gamma_1 = 1$$

(6b) $$\cos^2\alpha_2 + \cos^2\beta_2 + \cos^2\gamma_2 = 1$$

Similarly a lateral roentgenogram would give information about kyphosis or lordosis. From Fig 3 I get

(7) $$\phi = \gamma_3 + \gamma_4$$

Note that I am using A, B, C for posterio-anterior roentgeneogram and A_0, B_0 and C_0 for lateral roentgenogram. In principle these should be identical. I am using different symbols to allow for experimental errors. For Fig 3 eq. (5) takes the form

(8a,b) $\alpha_3+\gamma_3 = 90^0 = \alpha_4+\gamma_4, \qquad \beta_3 = 90^0 = \beta_4$

Therefore

(9a) $\cos^2\alpha_3 + \cos^2\beta_3 + \cos^2\gamma_3 = 1$

(9b) $\cos^2\alpha_3 + \cos^2\beta_3 + \cos^2\gamma_3 = 1$

The above are projections of spine in yz- and xz-planes. Considering spine in three dimensions (Fig 4), I have

(10) $\Omega_i = \gamma_i + \gamma_i'$

Ω_i is given the name 'Normal Asr Angle'(NAA). Using eq. (1) I can write

(11a) $\cos^2\alpha_i + \cos^2\beta_i + \cos^2\gamma_i = 1$

(11b) $\cos^2\alpha_i' + \cos^2\beta_i' + \cos^2\gamma_i' = 1$

The above angle is measured when the subject is standing. Now the subject is asked to hang freely from a bar in the wall and the angle is again measured after guarded graduated passive correction[3]. Let me denote 'Corrected Asr Angle' (CAA) as Ω_f. I can, therefore, write

(12) $\Omega_f = \gamma_f + \gamma_f'$

(13a) $\cos^2\alpha_f + \cos^2\beta_f + \cos^2\gamma_f = 1$

(13b) $\cos^2\alpha_f' + \cos^2\beta_f' + \cos^2\gamma_f' = 1$

Let $\psi = \langle R'A_1R$, $\psi' = \langle R'B_1R$ be the angles between the old and the new spinal positions. Using eq. (2) I can write (Fig 4)

(14a) $\cos\psi = \cos\alpha_i\cos\alpha_f + \cos\beta_i\cos\beta_f + \cos\gamma_i\cos\gamma_f$

(14b) $\cos\psi' = \cos\alpha_i'\cos\alpha_f' + \cos\beta_i'\cos\beta_f' + \cos\gamma_i'\cos\gamma_f'$

The degree of correction of spinal deformity can be defined as

(15) $D = 100(\sin\psi + \sin\psi')/(\sin\gamma_i + \sin\gamma_i')$

If the deformity is completely correctable $\psi = \gamma_i$, $\psi' = \gamma_i'$ and D = 100. If it is not correctable at all $\psi = \psi' = 0$ and D = 0. The deformity is classified as severe, intermediate or mild if D lies between 0-33.33, 33.34-66.66 or 66.67-100 respectively.

Consider Figures 4 and 5. Using eq. (3) I can write

(16a,b) $NA_0 = (A_1R)_{zx} = A_1R\sin\beta_i$; $OA = (A_1R)_{yz} = A_1R\sin\alpha_i$

(16c,d) $A_1S = (A_1R)_x = A_1R\cos\alpha_i$; $A_1T = (RA_1)_y = RA_1\cos\beta_i$

(16e) $CA = (A_1R)_z = A_1R\cos\gamma_i$

For an explanation of the symbols A, A_0 and A_1 see the note below eq. (7). From Figures 2 and 3 I have

(16f,g) $OA = AC/\cos\gamma_1$; $NA_0 = A_0C_0/\cos\gamma_3$

Comparing (16a,b) and (16f,g) I have

(17a,b) $AC/\cos\gamma_1 = RA\sin\alpha_i$; $A_0C_0/\cos\gamma_1 = RA_1\sin\beta_i$

Similarly I can write

(18a,b) $CB/\cos\gamma_2 = B_1 R\sin\alpha_i'$; $C_0B_0/\cos\gamma_4 = B_1 R\sin\beta_i'$

From Fig 5

(19a,b) $A_1T = OA\cos\beta_1$; $A_1S = NA_0\cos\alpha_3$

Using (16c,d) I get

(20a,b) $A_1R\cos\beta_i = OA\cos\beta_1$; $A_1R\cos\alpha_i = NA_0\cos\alpha_3$

Using (5a) and (16f) I have

(20c) $OA\cos\beta_1 = OA\sin\gamma_1 = AC\tan\gamma_1$

Therefore

(21a,b) $A_1R\cos\alpha_i = A_0C_0\tan\gamma_3$; $A_1R\cos\beta_i = AC\tan\gamma_1$

(22a,b) $RB_1\cos\alpha_i' = C_0B_0\tan\gamma_4$; $RB_1\cos\beta' = C_0B_0\tan\gamma_2$

In order to get rid of different scales, I introduce

(23) $P_1 = (AC + CB)/(A_0C_0 + C_0B_0)$

(24a,b) $A_1C_1 = P_1(A_0C_0)$; $C_1B_1 = P_1(C_0B_0)$

AC and A_0C_0 can now be replaced by A_1C_1. Similarly CB and C_0B_0 are replaced by C_1B_1. Equations (17), (18) and (21), (22) can, therefore, be written as

(25a,b) $A_1R\sin\alpha_i = A_1C_1\sec\gamma_1$; $A_1R\sin\beta_i = A_1C_1\sec\gamma_3$

(26a,b) $RB_1 \sin\alpha_i' = C_1 B_1 \sec\gamma_2$; $RB_1 \sin\beta_i' = C_1 B_1 \sec\gamma_4$

(27a,b) $A_1 R\cos\alpha_i = A_1 C_1 \tan\gamma_3$; $A_1 R\cos\beta_i = A_1 C_1 \tan\gamma_1$

(28a,b) $RB_1 \cos\alpha_i' = C_1 B_1 \tan\gamma_4$; $RB_1 \cos\beta_i' = C_1 B_1 \tan\gamma_2$

Therefore

(29a) $$A_1 R = A_1 C_1 (\tan^2\gamma_1 + 1 + \tan^2\gamma_3)^{\frac{1}{2}}$$

(29b) $$RB_1 = C_1 B_1 (\tan^2\gamma_2 + 1 + \tan^2\gamma_4)^{\frac{1}{2}}$$

which gives

(30a) $$\cos\alpha_i = \tan\gamma_3 / (\tan^2\gamma_1 + 1 + \tan^2\gamma_3)^{\frac{1}{2}}$$

(30b) $$\cos\alpha_i = \tan\gamma_1 / (\tan^2\gamma_1 + 1 + \tan^2\gamma_3)^{\frac{1}{2}}$$

Using eq. (11a) I get

(31a) $$\cos\gamma_i = (1 - \cos^2\alpha_i - \cos^2\beta_i)^{\frac{1}{2}}$$

which can be written as

(31b) $$\cos\gamma_i = (1 - \tan^2\gamma_1 - \tan^2\gamma_3)^{\frac{1}{2}} / (1 + \tan^2\gamma_1 + \tan^2\gamma_3)^{\frac{1}{2}}$$

Similarly

(32a) $$\cos\alpha_i' = \tan\gamma_4 / (\tan^2\gamma_2 + 1 + \tan^2\gamma_4)^{\frac{1}{2}}$$

(32b) $$\cos\beta_i' = \tan\gamma_2 / (\tan^2\gamma_2 + 1 + \tan^2\gamma_4)^{\frac{1}{2}}$$

Using eq. (11b) I get

(33a) $$\cos\gamma_i' = (1 - \cos^2\alpha_i' - \cos^2\beta_i')^{\frac{1}{2}}$$

which can be written as

$$(33b) \qquad \cos\gamma_i' = (1 - \tan^2\gamma_2 - \tan^2\gamma_4)^{\frac{1}{2}}/(1 + \tan^2\gamma_2 + \tan^2\gamma_4)^{\frac{1}{2}}$$

The measurements can be performed in the same way after guarded graduated passive correction. I can write the relations for the corrected angle as

$$(34a) \qquad \cos\alpha_f = \tan\gamma_3'/(\tan^2\gamma_1' + 1 + \tan^2\gamma_3')^{\frac{1}{2}}$$

$$(34b) \qquad \cos\beta_f = \tan\gamma_1'/(\tan^2\gamma_1' + 1 + \tan^2\gamma_3')^{\frac{1}{2}}$$

$$(34c) \qquad \cos\gamma_f = (1 - \cos^2\alpha_f - \cos^2\beta_f)^{\frac{1}{2}}$$

$$= (1 - \tan^2\gamma_1' - \tan^2\gamma_3')^{\frac{1}{2}}/(1 + \tan^2\gamma_1' + \tan^2\gamma_3')^{\frac{1}{2}}$$

$$(34d) \qquad \cos\alpha_f' = \tan\gamma_4'/(\tan^2\gamma_2' + 1 + \tan^2\gamma_4')^{\frac{1}{2}}$$

$$(34e) \qquad \cos\beta_f' = \tan\gamma_2'/(\tan^2\gamma_2' + 1 + \tan^2\gamma_4')^{\frac{1}{2}}$$

$$(34f) \qquad \cos\gamma_f' = (1 - \cos^2\alpha_f' - \cos^2\beta_f')^{\frac{1}{2}}$$

$$= (1 - \tan^2\gamma_2' - \tan^2\gamma_4')^{\frac{1}{2}}/(1 + \tan^2\gamma_2' + \tan^2\gamma_4')^{\frac{1}{2}}$$

The angles ψ and ψ' can now be found using eq. (14a,b). Eq. (15) will give the degree of correction of spinal deformity.

In order to measure these angles in a patient having spinal deformity, roentgenograms need to be taken at regular intervals. Also orthopedic problems cannot always be detected by inspection and physical examination only[4]. A full length standing roentgengenogram taken many times during the sensitive age period would result in too much radiation exposure to the children. During recent years, there has been much interest in using moiré fringe topography for the detection and documentation of scoliosis[5-9]. The technique of moiré topography consists of photographing the part of body to be studied through a specially constructed screen. Dark fringes

are produced on the body because of the presence of screen. The details of the the moiré technique are described elsewhere[10,11].

A relation for the measurement of the angle of spinal curvature from moiré topographs is derived elsewhere[11] and applied in different clinical situations[3,10]. Here the method is briefly described. Consider Fig 6. The angle of spinal curvature for a single curve scoliosis can be written as

$$\theta = \angle CAO + \angle CBO \tag{35}$$

To measure this angle, the midpoint of the neck P is joined to the midpoint of the waist Q. To find the position of the spine at a given point draw a line perpendicular to PQ. Let this line intersect PQ at C and a particular moiré fringe at H and E such that E is always on the right side of H. The midpoint O of the line segment HE gives the position of the spine, provided the positioning during the X-ray and moiré examinations is identical[11]. From the position of the spine at a given point, the distance to the line PQ is obtained as d = CO. The point where d is maximum is denoted by d_1. Considering C as the origin and taking the distance on the right as positive and that on the left as negative, d_1 can be written as

$$d_1 = \tfrac{1}{2}(CH + CE) \tag{36}$$

At point A above the point C on line PQ, where the moiré fringes show minimum asymmetry d should be minimum and is given by

$$d_2 = \tfrac{1}{2}(AD + AG) \tag{37}$$

At point B below the point C on the line PQ, where the moiré fringes show minimum asymmetry, the distance is given by

(38) $$d_3 = \tfrac{1}{2}(BF + BI)$$

Using eq. (4) this can be written as

(39a,b) $$\tan\gamma_1 = |d_1 - d_2|/AC; \qquad \tan\gamma_2 = |d_1 - d_3|/CB$$

The railroad sign line in Fig 6 represents the position of the spine. The way the angle is measured looks similar to Ferguson's method for measurements performed on the X rays.

The question now is which fringe should be chosen to perform the measurements. The fringes near the edge would be inappropriate because of edge effects. If the first fringe is chosen, measurement error would be more significant because CH and CE are small, Therefore a compromise has to be reached regarding the fringe chosen. Often it is difficult to find the exact point of maximum asymmetry. However, an area of asymmetry can be easily judged. El-Sayyad and I[3] suggested that measurements be taken at two points far below the point of maximum asymmetry and a line be drawn. Similarly measurements be taken at two points far above the point of maximum asymmetry and a line be drawn joining these points. The intersection of these lines would give the angle of spinal curvature which can be geometrically measured. The way the angle is measured looks similar to Cobb's method for measurements performed on the X rays.

Moiré topógraph of the side (with hand excluded) will give

information about kyphosis and lordosis. In this case d_1 is replaced by d_4, d_2 by d_5 and d_3 by d_6 (see Figures 2 and 8). Therefore

(40a,b) $\quad \tan\gamma_3 = |d_4 - d_5|/A_0C_0; \qquad \tan\gamma_4 = |d_4 - d_6|/C_0B_0$

Using (23), equations (39) and (40) can be written as

(41a,b) $\quad |d_1 - d_2| = A_1C_1\tan\gamma_1; \qquad |d_1 - d_3| = C_1B_1\tan\gamma_2$

(42a,b) $\quad |d_4 - d_5| = A_1C_1\tan\gamma_3; \qquad |d_4 - d_6| = C_1B_1\tan\gamma_4$

Using these in equations (30) and (32) I have

$$\text{(43a)} \quad \cos\alpha_i = |d_4 - d_5|/[(d_1 - d_2)^2 + (A_1C_1)^2 + (d_4 - d_5)^2]^{\frac{1}{2}}$$

$$\text{(43b)} \quad \cos\beta_i = |d_1 - d_2|/[(d_1 - d_2)^2 + (A_1C_1)^2 + (d_4 - d_5)^2]^{\frac{1}{2}}$$

$$\text{(44a)} \quad \cos\alpha_i' = |d_4 - d_6|/[(d_1 - d_3)^2 + (C_1B_1)^2 + (d_4 - d_6)^2]^{\frac{1}{2}}$$

$$\text{(44b)} \quad \cos\beta_i' = |d_1 - d_3|/[(d_1 - d_3)^2 + (C_1B_1)^2 + (d_4 - d_6)^2]^{\frac{1}{2}}$$

For the measurements performed after guarded graduated passive correction, I obtain

$$\text{(45a)} \quad \cos\alpha_f = |d_4' - d_5'|/[(d_1' - d_2')^2 + (A_1'C_1')^2 + (d_4' - d_5')^2]^{\frac{1}{2}}$$

$$\text{(45b)} \quad \cos\beta_f = |d_1' - d_2'|/[(d_1' - d_2')^2 + (A_1'C_1')^2 + (d_4' - d_5')^2]^{\frac{1}{2}}$$

$$\text{(46a)} \quad \cos\alpha_f' = |d_4' - d_6'|/[(d_1' - d_3')^2 + (C_1'B_1')^2 + (d_4' - d_6')^2]^{\frac{1}{2}}$$

$$\text{(46b)} \quad \cos\beta_f' = |d_1' - d_3'|/[(d_1' - d_3')^2 + (C_1'B_1')^2 + (d_4' - d_6')^2]^{\frac{1}{2}}$$

where

$$\text{(47)} \quad Q_1 = (A'C' + C'B')/(A_0'C_0' + C_0'B_0')$$

(48a,b) $\quad A_1'C_1' = Q_1(A_0'C_0'); \qquad B_1'C_1' = Q_1(B_0'C_0')$

Let me apply equations (45) and (46) to calculate the angle. Suppose the moiré fringe topograph of the back when the patient is standing looks like Fig 7. The following measurements are obtained:

$AD = 11.0$ mm, $AG = -21.0$ mm, $CH = 3.0$ mm, $CE = 9.0$ mm, $BF = 1.0$ mm, $BI = -5.0$ mm, $AC = 42.0$ mm, $CB = 20.0$ mm, $d_1 = \frac{1}{2}(CH + CE) = 6.0$ mm, $d_2 = \frac{1}{2}(AD + AG) = -5.0$ mm, $d_3 = \frac{1}{2}(BF + BI) = -2.0$ mm.

If the moiré topograph of the side in the standing position looks like Fig 8, I have

$A_0D_0 = 2.5$ mm, $A_0G_0 = -13.5$ mm, $C_0H_0 = -7.5$ mm, $C_0E_0 = 18.5$ mm, $B_0F_0 = 4.5$ mm, $B_0I_0 = -9.5$ mm, $A_0C_0 = 42.0$ mm, $C_0B_0 = 20.0$ mm, $d_4 = \frac{1}{2}(C_0H_0 + C_0E_0) = 5.5$ mm, $d_5 = \frac{1}{2}(A_0D_0 + A_0G_0) = -5.5$ mm, $d_6 = \frac{1}{2}(B_0F_0 + B_0I_0) = -2.5$ mm.

Substituting these values in (43a,b), (31a) and (44a,b), (33a), I get

$\cos\alpha_i = 0.2456$, $\cos\beta_i = 0.2456$, $\cos\gamma_i = 0.9377$,

$\cos\alpha_i' = 0.3482$, $\cos\beta_i' = 0.3482$, $\cos\gamma_i' = 0.8704$

Therefore

$\alpha_i = 75.78^0$, $\beta_i = 75.78^0$, $\gamma_i = 20.32^0$,

$\alpha_i' = 69.63^0$, $\beta_i' = 69.63^0$, $\gamma_i' = 29.50^0$,

$\Omega_i = \gamma_i + \gamma_i' = 49.82^0$.

Let the moiré topographs of the back and side when the patient is hanging freely from a bar in the wall look like Figures 9 and 10. The following measurements are obtained

$A'D' = 11.0$ mm, $A'G' = -21.0$ mm, $C'H' = 4.0$ mm, $C'E' = 6.0$ mm, $B'F' = 1.0$ mm, $B'I' = -5.0$ mm, $A'C' = 42.0$ mm, $C'B' = 2.0$ mm, $d_1' = \frac{1}{2}(C'H' + C'E') = 5.0$ mm, $d_2' = \frac{1}{2}(A'D' + A'G') = -5.0$ mm, $d_3' = \frac{1}{2}(B'F' + B'I')$

= -2.0 mm, $A_0'D_0'$ = 2.5 mm, $A_0'G_0'$ = -13.5 mm, $C_0'H_0'$ = -7.5 mm, $C_0'E_0'$ = 16.5 mm, $B_0'F_0'$ = 4.5 mm, $B_0'I_0'$ = -9.5 mm, $A_0'C_0'$ = 42.0 mm, $C_0'B_0'$ = 20.0 mm, $d_4' = \frac{1}{2}(C_0'H_0' + C_0'E_0') = 4.5$ mm, $d_5' = \frac{1}{2}(A_0'D_0' + A_0'G_0') = -5.5$ mm, $d_6' = \frac{1}{2}(B_0'F_0' + B_0'I_0') = -2.5$ mm.

Therefore

$\cos\alpha_f = 0.2256$, $\cos\beta_f = 0.2256$, $\cos\gamma_f = 0.9477$,

$\cos\alpha_f' = 0.3137$, $\cos\beta_f' = 0.3137$, $\cos\gamma_f' = 0.8962$,

$\alpha_f = 76.96^0$, $\beta_f = 76.96^0$, $\gamma_f = 18.60^0$,

$\alpha_f' = 71.62^0$, $\beta_f' = 71.62^0$, $\gamma_f' = 26.33^0$,

$\Omega_f = \gamma_f + \gamma_f' = 44.93^0$, $\cos\psi = 0.9995$, $\cos\psi' = 0.9985$, D = 10.28.

The same calculation done using fortran program ASR.FOR gives D = 10.13. Therefore the deformity is classified as 'severe'. The fortran program ASR.FOR is given in the appendix.

The moiré topographic technique offers numerous possibilities in the documenatation of orthopedic defects. The possibility of physio-theraputic improvement of back deformity can now be quantitatively determined by taking a moiré topograph of the patient (in the normal and hanging positions). The same procedure can also be applied for the deformities of lower limbs. The method and elaboration here reported provides the necessary basis for a correct diagnosis and prognosis of back deformities. It also offers a means of determining the effectiveness of treatment. It is hoped that with accurate measurements performed on the moiré topographs, X rays will not be needed for the measurement of the angle of spinal curvature.

I would like to thank Dr. Mohsen M. El-Sayyad for suggesting me to treat the spinal problem in three dimensions.

APPENDIX: FORTRAN PROGRAM FOR THE CALCULATION OF ASR ANGLE

```
C ASR.FOR
C THIS PROGRAM COMPUTES ASR ANGLE FROM MOIRE TOPOGRAPHS
C ALL RIGHTS RESERVED. THIS PROGRAM CANNOT BE REPRODUCED OR RUN WITHOUT
C PRIOR PERMISSION FROM S ARIF KAMAL
C ALL LENGTHS ARE IN MM
C ANGLES ARE CALCULATED IN DEGREES
C VARIABLES ENDING WITH AN "A" ARE FOR BACK MEASUREMENTS IN NORMAL POSITION
C VARIABLES ENDING WITH A "B" ARE FOR SIDE MEASUREMENTS IN NORMAL POSITION
C VARIABLES ENDING WITH A "C" ARE FOR BACK MEASUREMENTS IN CORRECTED POSITION
C VARIABLES ENDING WITH A "D" ARE FOR SIDE MEASUREMENTS IN CORRECTED POSITION
C VARIABLES ENDING WITH A "U" ARE FOR UPPER PORTION IN NORMAL POSITION
C VARIABLES ENDING WITH A "L" ARE FOR LOWER PORTION IN NORMAL POSITION
C VARIABLES ENDING WITH A "V" ARE FOR UPPER PORTION IN CORRECTED POSITION
C VARIABLES ENDING WITH A "M" ARE FOR LOWER PORTION IN CORRECTED POSITION
C THE FOLLOWING COMMANDS SHOULD BE USED FOR CREATING FILES AND RUNNING PROGRAM
C CR ASRDAT.DAT(ENTER DATA), CR ASROUT.OUT, FOR ASR, LINK ASR
C ASSIGN ASRDAT.DAT FOR$READ, ASSIGN ASROUT.OUT FOR$PRINT, RUN ASR.EXE
C TO TERMINATE THE PROGRAM ENTER -1, 1.0, 1.0, . . . . , 1.0 IN ASRDAT.DAT
C OUTPUT WOULD BE OBTAINED BY PRINTING ASROUT.OUT
      REAL NAA,KA,LA,KB,LB,KC,LC,KD,LD
      CHARACTER*3 C0, C1, C2, C3, C4, C5, C6, C7, C8
      CHARACTER*3     C9, C10, C11, C12, C13, C14, C15, C16
      CHARACTER*3     C17, C18, C19, C20, C21, C22, C23, C24
      CHARACTER*3     C25, C26, C27, C28, C29, C30, C31, C32
      CHARACTER*14 CLASS
      CHARACTER*4 M
      READ 4, M
4     FORMAT (A7)
      READ 5, C0, C1, C2, C3, C4, C5, C6, C7, C8
5     FORMAT (A4, A5, 7A6)
      READ 6,     C9, C10, C11, C12, C13, C14, C15, C16
6     FORMAT (A9, 7A6)
      READ 7,     C17, C18, C19, C20, C21, C22, C23, C24
7     FORMAT (A9, 7A6)
      READ 8,     C25, C26, C27, C28, C29, C30, C31, C32
8     FORMAT (A9, 7A6)
      PRINT*, '
      PRINT*, '
      PRINT*, '
      PRINT*, 'CALCULATION OF ASR ANGLE'
      PRINT*, '
      PRINT*, '
      PRINT 9
9     FORMAT (' SURGICAL TREATMENT IS RECOMMENDED IN CASE OF SEVERE
     +DEFORMITY')
      PRINT*, '
      PRINT 11
11    FORMAT (' BRACE TREATMENT IS RECOMMENDED IN CASE OF INTERMEDIATE
     + DEFORMITY')
      PRINT*, '
      PRINT 12
12    FORMAT (' EXERCISE TREATMENT IS RECOMMENDED IN CASE OF MILD
     +DEFORMITY')
      PRINT*, '
      PRINT*, '
      PRINT*, 'MOIRE TOPOGRAPH NUMBER: N'
      PRINT*, 'NORMAL ASR ANGLE (DEGREES): NAA'
      PRINT*, 'CORRECTED ASR ANGLE (DEGREES): CAA'
      PRINT*, 'DEGREE OF CORRECTION OF DEFORMITY: D'
      PRINT*, '
      PRINT 10
10    FORMAT (4X,'N',8X,'NAA',9X,'CAA',10X,'D',9X,'CLASSIFICATION')
```

```
      PRINT*,  '          '
20    READ*, N, AGA, ADA, CHA, CEA, BIA, BFA, ACA, CBA
      READ*,    AGB, ADB, CHB, CEB, BIB, BFB, ACB, CBB
      READ*,    AGC, ADC, CHC, CEC, BIC, BFC, ACC, CBC
      READ*,    AGD, ADD, CHD, CED, BID, BFD, ACD, CBD
        IF (N.LT.0) GO TO 40
        XA = (CHA + CEA)/2
        YA = (ADA + AGA)/2
        ZA = (BFA + BIA)/2
        XB = (CHB + CEB)/2
        YB = (ADB + AGB)/2
        ZB = (BFB + BIB)/2
        XC = (CHC + CEC)/2
        YC = (ADC + AGC)/2
        ZC = (BFC + BIC)/2
        XD = (CHD + CED)/2
        YD = (ADD + AGD)/2
        ZD = (BFD + BID)/2
         P = (ACA + CBA)/(ACB + CBB)
         Q = (ACC + CBC)/(ACD + CBD)
        KA = ABS(XA - YA)
        LA = ABS(XA - ZA)
        KB = (ABS(YB - XB))*P
        LB = (ABS(XB - ZB))*P
        KC = ABS(XC - YC)
        LC = ABS(XC - ZC)
        KD = (ABS(XD - YD))*Q
        LD = (ABS(XD - ZD))*Q
        CSAU = KB/(SQRT((KA**2) + (ACA**2) + (KB**2)))
        CSBU = KA/(SQRT((KA**2) + (ACA**2) + (KB**2)))
        CSCU = SQRT(1 - (CSAU**2) - (CSBU**2))
        CSAL = LB/(SQRT((LA**2) + (CBA**2) + (LB**2)))
        CSBL = LA/(SQRT((LA**2) + (CBA**2) + (LB**2)))
        CSCL = SQRT(1 - (CSAL**2) - (CSBL**2))
        CSAV = KD/(SQRT((KC**2) + (ACC**2) + (KD**2)))
        CSBV = KC/(SQRT((KC**2) + (ACC**2) + (KD**2)))
        CSCV = SQRT(1 - (CSAV**2) - (CSBV**2))
        CSAM = LD/(SQRT((LC**2) + (CBC**2) + (LD**2)))
        CSBM = LC/(SQRT((LC**2) + (CBC**2) + (LD**2)))
        CSCM = SQRT(1 - (CSAM**2) - (CSBM**2))
        CSSU = (CSAU*CSAV) + (CSBU*CSBV) + (CSCU*CSCV)
        CSSL = (CSAL*CSAM) + (CSBL*CSBM) + (CSCL*CSCM)
          SU = ACOS(CSSU)
          SL = ACOS(CSSL)
          CU = ACOS(CSCU)
          CL = ACOS(CSCL)
          CV = ACOS(CSCV)
          CM = ACOS(CSCM)
         NAA = (CU + CL)*180/3.14159
         CAA = (CV + CM)*180/3.14159
           D = 100*(SIN(SU) + SIN(SL))/(SIN(CU) + SIN(CL))
        IF (D .LE. 33.34) THEN
          CLASS = '    SEVERE    '
        ELSE IF (D .LE. 66.67) THEN
          CLASS = ' INTERMEDIATE '
        ELSE
          CLASS = '     MILD     '
        END IF
        PRINT 30, N, NAA, CAA, D, CLASS
30      FORMAT (1X, I4, 7X, F5.2, 7X, F5.2, 7X, F5.2, 7X, A14)
        GO TO 20
40      STOP
        END
```

```
DATA
 N   AGA    ADA    CHA    CEA    BIA    BFA    ACA    CBA
     AGB    ADB    CHB    CEB    BIB    BFB    ACB    CBB
     AGC    ADC    CHC    CEC    BIC    BFC    ACC    CBC
     AGD    ADD    CHD    CED    BID    BFD    ACD    CBD

 1 -21.0   11.0    3.0    9.0   -5.0    1.0   42.0   20.0
   -13.5    2.5   -7.5   18.5   -9.5    4.5   42.0   20.0
   -21.0   11.0    4.0    6.0   -5.0    1.0   42.0   20.0
   -13.5    2.5   -7.5   16.5   -9.5    4.5   42.0   20.0
-1   1.0    1.0    1.0    1.0    1.0    1.0    1.0    1.0
     1.0    1.0    1.0    1.0    1.0    1.0    1.0    1.0
     1.0    1.0    1.0    1.0    1.0    1.0    1.0    1.0
     1.0    1.0    1.0    1.0    1.0    1.0    1.0    1.0
```

CALCULATION OF ASR ANGLE

SURGICAL TREATMENT IS RECOMMENDED IN CASE OF SEVERE DEFORMITY

BRACE TREATMENT IS RECOMMENDED IN CASE OF INTERMEDIATE DEFORMITY

EXERCISE TREATMENT IS RECOMMENDED IN CASE OF MILD DEFORMITY

MOIRE TOPOGRAPH NUMBER: N
NORMAL ASR ANGLE (DEGREES): NAA
CORRECTED ASR ANGLE (DEGREES): CAA
DEGREE OF CORRECTION OF DEFORMITY: D

N	NAA	CAA	D	CLASSIFICATION
1	49.82	44.94	10.13	SEVERE

[1]M. O. Tachdjian, Pediatric Orthopedics, Vol. 2 (Saunders, Philadelphia, 1972), pp. 1201-2.

[2]'Asr' (Arabic) means frame, and is taken from the following verse of Al-Quran:

نَحْنُ خَلَقْنٰهُمْ وَشَدَدْنَآ اَسْرَهُمْ ۚ وَاِذَا شِئْنَا بَدَّلْنَآ
اَمْثَالَهُمْ تَبْدِيْلًا ﴿٢٨﴾

'We, even We created them and strengthened their frame. And when We will, We can replace them, bringing others like them in their stead.' (Sura 76:28).

[3]M. M. El-Sayyad and S. A. Kamal, Cobb's angle measurement by moiré topographs, Proc. 34th Ann. Conf. Eng. Med. Biol. 23(1981)311.¥

[4]R. B. Winter, Modern Medicine, May 1, 1975, p. 38.

[5]I. V. Adair, M. C. van Wijk and G. W. D. Armstrong, Clin. Orthop. 129(1977)165.

[6]S. A. Kamal and M. A. Khan, Moiré contour recorder, 19th Annual Science Conference, Quaid-e-Azam University, Islamabad (Pakistan), 1979.ξ

[7]S. Willner, Acta Orthop. Scand. 50(1979)295.

[8]S. A. Kamal and M. M. El-Sayyad, The use of moiré topographs for the detection of orthopedic defects in children of age group four to seven years, 23rd Annual Meeting of the American Association of Physicists in Medicine, Boston, Ma.; Med. Phys. 8(1981) 549.£

[9]M. S. Moreland, M. H. Pope and G. W. D. Armstrong, Moiré Fringe Topography and Spinal Deformity (Pergamon, New York, 1981).

[10]S. A. Kamal and R. E. Lindseth, Moiré topography for the detection of orthopedic defects, Periodic Structures, Gratings, Moiré Patterns and Diffraction Phenomena, Proc. Soc. Photo-Opt. Instr. Eng. 240(1980)293.θ

[11]S. A. Kamal, J. Islamic Med. Assoc.(USA) 14(1982)146.€

¥ Full text: https://www.ngds-ku.org/Papers/C12.pdf
£ Full text: https://www.ngds-ku.org/Papers/C11.pdf
€ Full text: https://www.ngds-ku.org/Papers/J04.pdf
ξ Full text: https://www.ngds-ku.org/Papers/C04.pdf
θ Full text: https://www.ngds-ku.org/Papers/C08.pdf

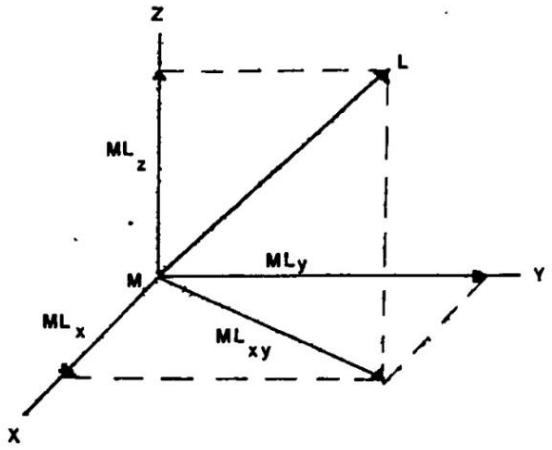

Fig 1. A vector in three dimensions

In Fig 4.

$\alpha_i = \angle XA_1R$

$\alpha_i' = \angle X'B_1R$

$\beta_i = \angle YA_1R$

$\beta_i' = \angle Y'B_1R$

$\gamma_i = \angle B_1A_1R$

$\gamma_i' = \angle A_1B_1R$

$\alpha_f = \angle XA_1R'$

$\alpha_f' = \angle X'B_1R'$

$\beta_f = \angle YA_1R'$

$\beta_f' = \angle Y'B_1R'$

$\gamma_f = \angle B_1A_1R'$

$\gamma_f' = \angle A_1B_1R'$

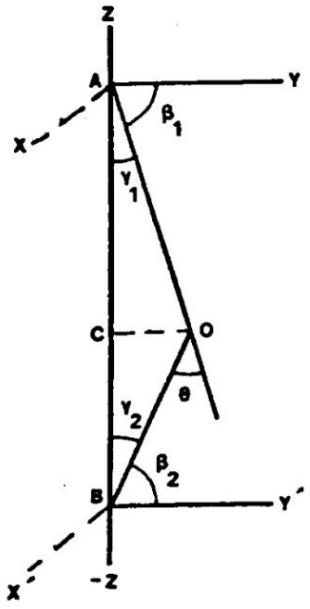

Fig 2. Projection of spine in yz-plane

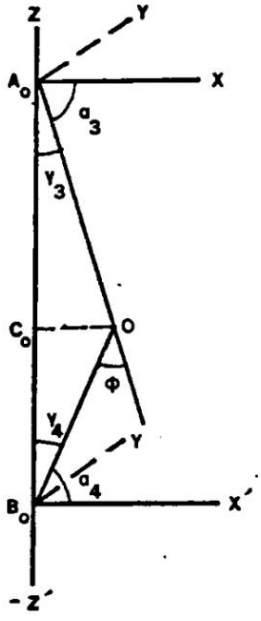

Fig 3. Projection of spine in xz-plane

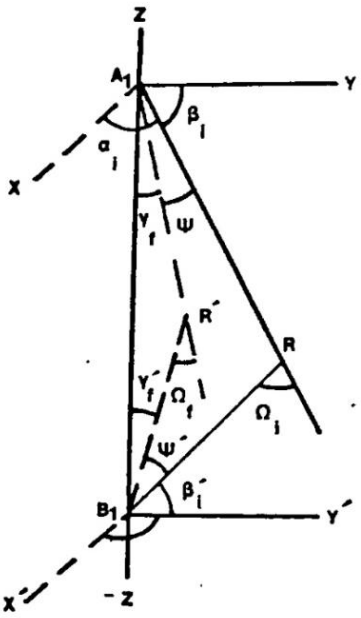

Fig 4. Spine in three dimensions

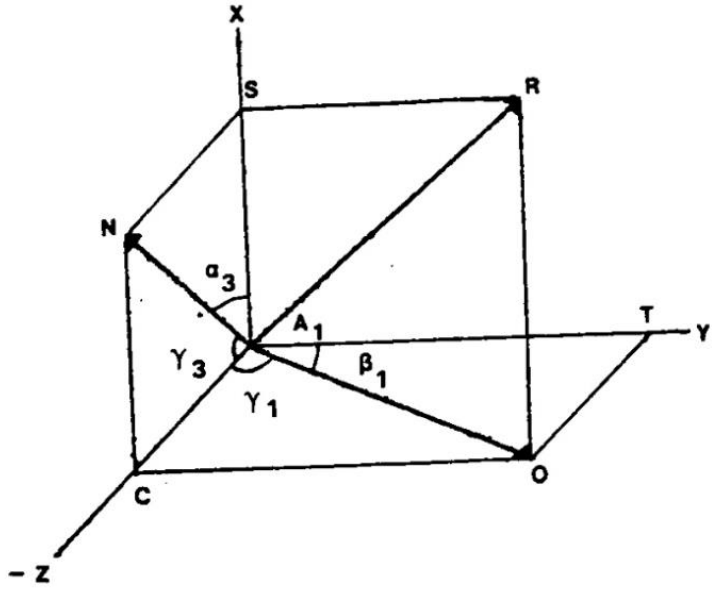

Fig 5. Projections of a vector in yz- and xz-planes

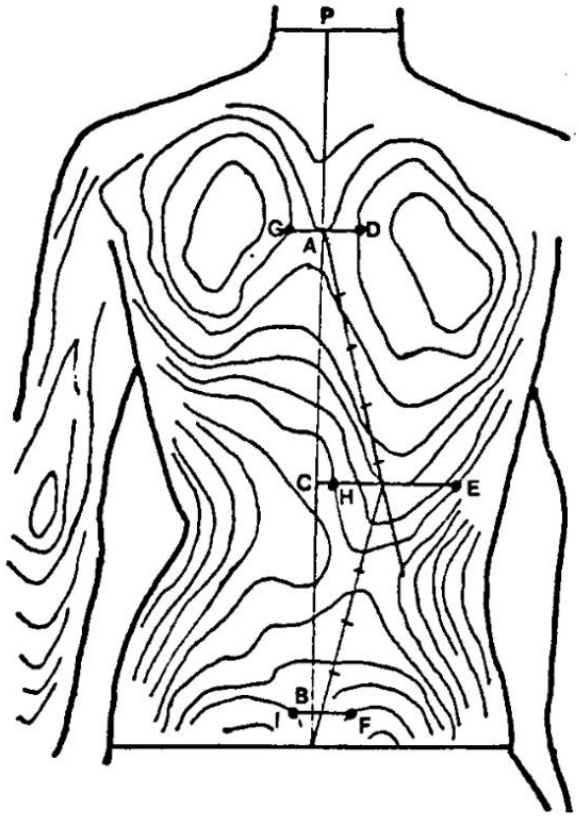

Fig 6. Measurement of the angle of spinal curvature by moiré topographs

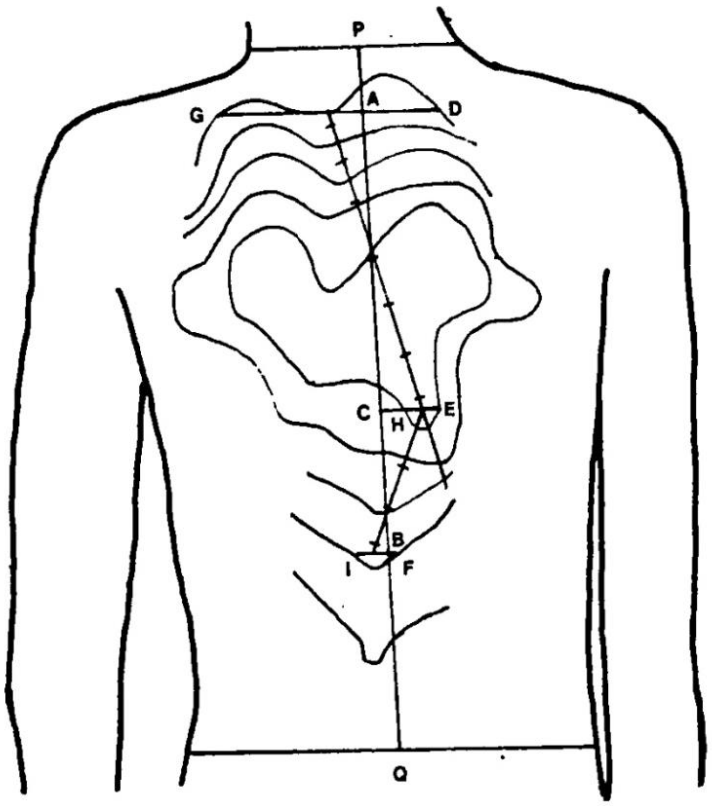

Fig 7. Moiré topograph of the back in the standing position

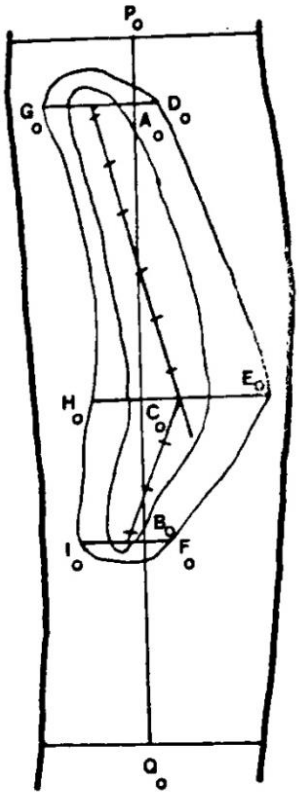

Fig 8. Moiré topograph of the side in the standing position

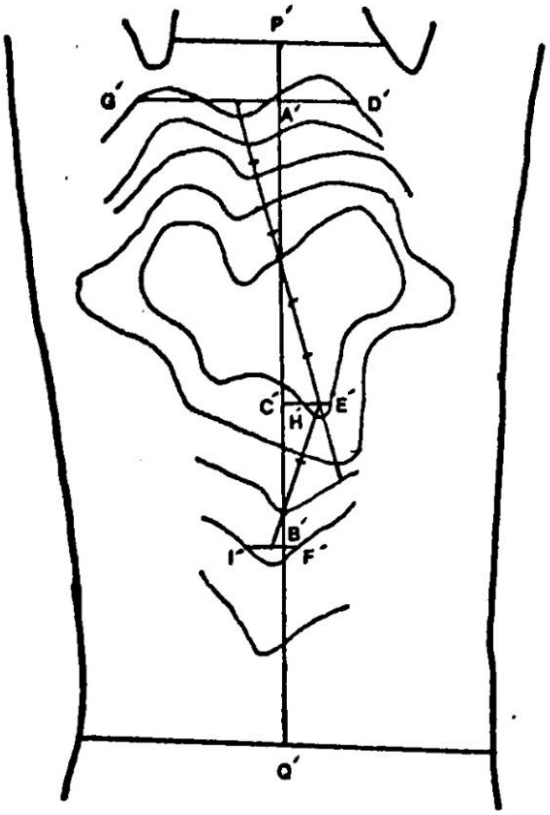

Fig 9. Moiré topograph of the back after passive correction

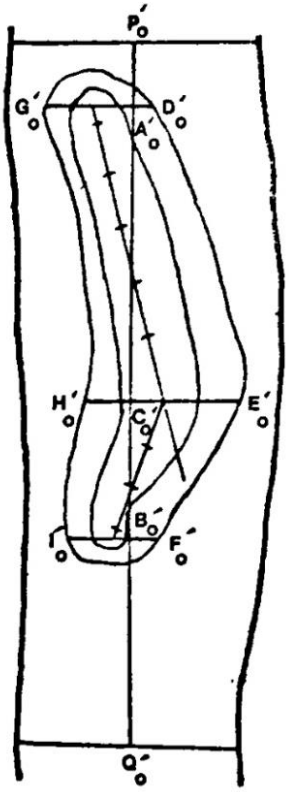

Fig 10. Moiré topograph of the side after passive correction